Amino Acids (2010) 38:1583–1593
DOI 10.1007/s00726-009-0378-9

ORIGINAL ARTICLE

Subcellular localization of the interaction between the human immunodeficiency virus transactivator Tat and the nucleosome assembly protein 1

Alex De Marco · Pablo D. Dans · Anna Knezevich · Paolo Maiuri · Sergio Pantano · Alessandro Marcello

Received: 17 August 2009 / Accepted: 14 October 2009 / Published online: 4 November 2009

Abstract The histone chaperone nucleosome assembly protein, hNAP-1, is a host cofactor for the activity of the human immunodeficiency virus type 1 (HIV-1) transactivator Tat. The interaction between these two proteins has been shown to be important for Tat-mediated transcriptional activation and for efficient viral infection. Visualization of HIV-1 transcription and fluorescence resonance energy transfer experiments performed in this work demonstrate that hNAP-1 is not recruited to the site of Tat activity but the two proteins interact at the nuclear rim. These data are consistent with a mechanism that requires hNAP-1 for the transport of Tat within the nucleus rather than for the remodeling of nucleosomes on the provirus. Protein–protein docking and molecular modeling of the complex suggest that this interaction occurs between the basic domain of Tat and the histone-binding domain. The combination of theoretical and whole cell studies provided new insights into the functional significance of the Tat:hNAP-1 recognition.

A. De Marco · A. Knezevich · P. Maiuri · A. Marcello (✉)
Laboratory of Molecular Virology,
International Centre for Genetic Engineering and Biotechnology (ICGEB), Padriciano, 99, 34012 Trieste, Italy
e-mail: marcello@icgeb.org
URL: http://www.icgeb.org/molecular-virology.html

P. D. Dans · S. Pantano
Biomolecular Simulations Group,
Institut Pasteur of Montevideo, Calle Mataojo 2020,
CP 11400 Montevideo, Uruguay

Present Address:
A. De Marco
European Molecular Biology Organization (EMBL),
Meyerhofstraße 1, 69117 Heidelberg, Germany

Keywords HIV · Chromatin · hNAP-1 · FRET · Protein interaction

Introduction

The nucleosome is the core structural unit of eukaryotic chromatin. It consists of two copies each of the four core histones H2A, H2B, H3 and H4 that form the histone octamer, around which the DNA is wrapped (Luger et al. 1997). The nucleosome is not only a structural unit of the chromosome but also a key hub for the signals that regulate nuclear processes such as replication, gene expression and repair (Groth et al. 2007; Li et al. 2007). Chromatin architectural states can be modulated by enzymatic modifications of histones and by the incorporation of histone variants by active remodeling of chromatin (Kouzarides 2007). Histones are highly basic proteins and require protein chaperones that facilitate their proper interaction with a specific chromatin location, but also prevent them from making unwanted interactions with other proteins or with DNA (Park and Luger 2006a). A number of histone chaperones are involved in chromatin assembly, in conjunction with ATP-dependent chromatin remodeling factors (Haushalter and Kadonaga 2003). Among them, hNAP1 was originally identified in HeLa cells as the human homolog of the yeast nucleosome assembly protein 1 (yNAP-1) that is the most characterized member of the family (Ishimi and Kikuchi 1991). In addition to its role as a chromatin-assembly factor and histone-storage protein, NAP-1 has been implicated in cell-cycle regulation (Kellogg et al. 1995), transcription regulation (Walter et al. 1995), incorporation and exchange of histone variants (Levchenko and Jackson 2004; Mizuguchi et al. 2004; Okuwaki et al. 2005), the promotion of nucleosome sliding

(Park et al. 2005) and the shuttling of histones into the nucleus (Ito et al. 1996).

The human immunodeficiency virus type 1 (HIV-1) is a retrovirus that requires integration of its genome into the chromatin of the infected cell. A key step in the regulation of HIV-1 gene expression is the activity of the viral Tat *trans*-activator. Tat is a small polypeptide that binds the 5′ end of all viral messenger RNAs via a *cis*-acting RNA element called the transactivation-responsive region TAR (Berkhout et al. 1989). Tat activates transcription from the HIV long terminal repeat (LTR) by integrating several host coactivators of transcription including p300, the p300/CBP-associated factor (P/CAF) and the positive transcription-elongation complex (P-TEFb) (Marcello et al. 2001b). Tat is a basic protein that is subject of many post-translational modifications typical of histones including: acetylation, methylation, phosphorylation and ubiquitylation. These modifications affect the activity of Tat in several ways. For example, the p300/CBP-associated factor (P/CAF) acetyltransferase binds to acetylated Tat at Lysine 50 and acetylates Lys28 (Bres et al. 2002; Dorr et al. 2002; Kiernan et al. 1999; Ott et al. 1999). Acetylation at Lys50 is mediated by the p300 coactivator that is also involved in histone acetylation at the HIV-1 LTR to promote transcription (Benkirane et al. 1998; Hottiger and Nabel 1998; Marzio et al. 1998). Subsequent steps of acetylation/deacetylation control the association of Tat with P-TEFb and TAR (Pagans et al. 2005). In addition, arginine methylation of Tat negatively affects Tat-TAR-cyclin T1 ternary complex formation and diminishes cyclin T1-dependent Tat transcriptional activation (Xie et al. 2007). However, how these complexes are temporally and spatially regulated in the living cell remains debated. One model suggests that P-TEFb remains associated with Tat to the elongating RNA polymerase II (RNAPII) (Bres et al. 2002, 2005; Ping and Rana 2001). Alternatively, P-TEFb dissociates from the elongating complex while Tat and P/CAF remain associated (Kaehlcke et al. 2003). However, analysis of the rates of association/dissociation of the TAR:Tat:P-TEFb complex in living cells, by performing fluorescence recovery after photobleaching experiments at the HIV-1 transcription sites, demonstrated that while RNAPII remains associated for the time required for transcription of the whole viral genome, as expected for the processing enzyme, Tat and P-TEFb undergo continuous cycles of association/dissociation (Boireau et al. 2007; Molle et al. 2007). Hence, transcription from the HIV-1 provirus is a dynamic process that requires a continuous exchange of factors rather than a stepwise ordered assembly. Understanding of the spatial regulation of HIV transcription by the visualization of subnuclear dynamics of the proteins involved in this process and the study of their reciprocal interactions can be obtained by the exploitation of high-resolution microscopy approaches for the visualization of proteins labeled with fluorescent tags (Marcello et al. 2004). In particular, protein–protein interactions can be visualized in a single cell by fluorescence (Förster) resonance energy transfer (FRET) (Marcello et al. 2001a). FRET is a mechanism of non-radiative transfer of energy between two fluorescent chromophores when in close proximity (typically less than 10 nm) (Day et al. 2001). FRET presents several advantages in comparison with other techniques employed to detect protein–protein interactions. Since FRET actually indicates protein–protein interaction at distances of a few nanometers, the simple co-localization of two proteins is not sufficient to yield energy transfer. Furthermore, the use of gene-encoded green fluorescent protein (GFP) variants allows also the visualization of the interactions in real time and in living cells, particularly using FRET-dependent fluorescence lifetime imaging microscopy (Voss et al. 2005). Therefore, FRET can be used to determine if, when and where specific protein pairs interact inside the cell. This is of particular value since most biological processes occur within discrete functional subcellular compartments in vivo (Cook 1999; Sutherland and Bickmore 2009).

The histone chaperone hNAP-1 has been found to be a novel cellular protein interacting with HIV-1 Tat (Vardabasso et al. 2008). hNAP-1 significantly enhanced Tat-mediated activation of the LTR and viral infection. Conversely, knockdown of hNAP-1 decreased viral activity. In this work, we explored whether hNAP-1 is enriched with Tat at the site of HIV-1 transcription by two complementary approaches. hNAP-1 could not be detected at the site of HIV-1 RNA biogenesis, where instead both Tat and associated factors like Cyclin T1 were enriched. However, we could visualize the interaction of hNAP-1 and Tat by FRET within the nuclear rim.

In an attempt to gain structural insights, we sought to construct a structural model of the adduct. In support to our hypothesis, protein–protein docking suggests that the basic domain of Tat specifically recognizes the histone-binding site of hNAP-1. Hence, we conclude that hNAP-1 acts by chaperoning Tat into the nucleus rather than being recruited by Tat at the site of transcription for histone remodeling purposes.

Materials and methods

Cells, plasmids and siRNA

Cells were cultivated at 37°C in Dulbecco's modified Eagle medium (DMEM) containing 10% FCS and antibiotics. U2OS HIV_Exo_24 × MS2 cells were obtained as described (Boireau et al. 2007). Plasmid transfections were

done using Lipofectamin (Invitrogen Ltd, Paisley, UK). Treatment with Leptomycin B was for 4 h at 40 ng/ml.

Plasmids encoding tagged versions of HIV-1 Tat, MS2 and ANP32B were previously described (Boireau et al. 2007; Marcello et al. 2001a). The FRET control plasmids encoding CFP-YFP and ANP32B-YFP were generated by PCR as described (Karpova et al. 2003; Pegoraro et al. 2006).

The mutated construct hNAP-EYFP* was constructed by PCR into pEYFP-N1 (Clontech Laboratories, Mountain View, CA, USA) between the *Hin*dIII and *Bam*HI restriction sites. The mutations of the siRNA target site involved only the DNA sequence, with no modifications at the aminoacidic level.

RNA interference (RNAi) for hNAP-1 was performed against the target sequence 5′ AAGGAACACGAUGAA CCUAUU 3′. An siRNA targeted against the GFP RNA was used as a control (5′ GGCTACGTCCAGGAGCGC ACC 3′). Synthetic double-stranded RNA oligonucleotides were purchased from Dharmacon. The RNAi transfections were done using Oligofectamin (Invitrogen) according to manufacturers' protocols as described (Vardabasso et al. 2008).

Luciferase assay

A reporter cell line containing a single copy of the integrated HIV-1 LTR-luciferase reporter construct (HeLa LTR-Luc) was used (du Chene et al. 2007). Transactivation with GST-Tat was carried out as previously described (Lusic et al. 2003). Luciferase activity was measured 48 h after transduction according to the manufacturer's protocol (Promega Corporation, Madison, WI, USA). Luciferase activity was normalized to protein concentration using Bradford (Bio-Rad Laboratories, Segrate (MI), Italy).

Immunofluorescence, image acquisition and FRET

Anti-hNAP-1 mouse monoclonal antiserum was a kind gift from Y. Ishimi (Ishimi and Kikuchi 1991). Mouse monoclonal anti-tubulin was purchased from Sigma. Immunofluorescence was performed as described with 1/10 dilution of the anti-hNAP-1 antibody (Marcello et al. 2003).

FRET analyses were performed in two ways in order to have a double check and a more precise measure of the FRET efficiency. The first approach consisted in the acquisition of the emission spectra from cells co-transfected with ECFP and EYFP-conjugated proteins when excited at 405 nm. The analyses of the resulting spectra have been conducted using Matlab (MathWorks, Natick, MA, USA) and the FRET efficiency calculated as the difference in the ratio between the signal at 524 nm and the signal at 502 nm. The spectra where previously normalized for the signal at 470 nm. The second approach consisted in three subsequent steps. First, cells co-transfected with ECFP and EYFP fusion proteins have been imaged in order to get the signal from the ECFP (em. 470–502 nm, ex. 405 nm). Then the cells have been imaged for the EYFP signal (em. 524–530 nm, ex. 514 nm). Third, images have been collected to get the EYFP signal when excited using the ECFP settings (em. 524–530 nm, ex. 405 nm). Analyses of data were done using the ImageJ PlugIn 'PixFRET' (Feige et al. 2005).

The Image acquisitions for immunofluorescence and FRET experiments were performed using a confocal microscope (Zeiss LSM510-META) with a 100× NA 1.4 objective.

Computational details

The starting model of the fusion protein Tat-fluorescent module used as one of the docking partners was constructed from: (1) the NMR structure of the Tat variant Bru (PDB code: 1JFW model 8) (Peloponese et al. 2000). This is the more similar variant to the strain used in our experiments, for which the structure has been solved; (2) the structure of the Yellow Fluorescent Protein (PDB code: 1YFP) (Wachter et al. 1998). Note that the fluorescent protein was included only to explicitly consider the gross steric hindrance in the docking. Therefore, the minor differences with the actual sequence used in the FRET experiments are not likely to influence the results. The model of the Tat-YFP fusion protein was constructed and structurally relaxed by molecular dynamics simulations using a previously established procedure (Pantano 2008). The second docking partner was the X-ray structure of the yeast variant of hNAP-1 (PDB code: 2AYU) (Park and Luger 2006b). Since the last 44 residues are missing in the X-ray structure of yeast NAP-1, we conducted a series of MD-based simulated annealing simulations to estimate the average distance between the last residues determined by crystallography and the YFP fluorophore. Due to the roughness of the information obtained from this technique, the position of these residues were not included in the docking. This information was only used to get an approximate gauge of the geometrical determinants between the donor–acceptor FRET pair (see "Results"). MD Simulations were performed using the generalized Born (GB) model for implicit solvation as implemented in Amber (Case et al. 2004; Cornell et al. 1995). The standard implementation (Hawkins et al. 1996) and parameters (Tsui and Case 2000) were used (option igb = 1 in the sander module of the Amber package). A cutoff radius of 1.8 nm and the Amber99 parameterization were adopted. The SHAKE method (Ryckaert et al. 1977) was used to constrain all the bonded interactions involving hydrogen atoms after energy minimization. A thermalization period of 2 ns

was adopted, in which the systems were heated up from 0 to 298 K using loose harmonic restraints of 5 Kcal/mol Å^2. After that point, production runs of 18 ns, without restraints, was performed and recorded for analysis every 2 ps. Docking runs were performed using Hex 5.1 (http://www.csd.abdn.ac.uk/hex/) (Ritchie 2008). The rigid rotational search was performed with the 3D FFT algorithm using a 0.6 Å grid taking into account the proteins shape and electrostatic. For two NAP-1:Tat-CFP initial conformations, ~60,000 possible orientations were computed. Top 2,000 docking solutions were then retained for which Newton-like energy minimizations were applied. These energies were calculated using "soft" Lennard-Jones and hydrogen bond potentials, adapted from the OPLS force-field parameters, along with an explicit charge–charge electrostatic contribution.

Results

Characterization of hNAP-1-YFP*

In order to study the dynamic behavior of hNAP-1 we generated a fusion construct with the enhanced yellow fluorescent protein (YFP). In order to avoid overexpression artefacts in the analyses, we wanted to substitute ectopically expressed hNAP-1 to the endogenous one. Therefore, taking advantage of a very efficient siRNA designed previously (Vardabasso et al. 2008), we mutagenized its target site in the hNAP-1 cDNA of the hybrid construct (hNAP-YFP*) (Fig. 1a). The construct showed the expected size and was resistant to a siRNA against hNAP1 (Fig. 1b). In order to establish if the hybrid construct carrying the additional YFP moiety was functional, we used the reporter cell line HeLa LTR-Luc that responds to Tat transactivation. As shown in Fig. 1c, the effect of the knockdown of endogenous hNAP-1 on Tat transactivation could be rescued by hNAP-YFP*.

The subcellular localization of hNAP-1 was analyzed in HeLa cells by immunofluorescence against hNAP-1. As shown in Fig. 2a, hNAP-1 staining appears mostly cytoplasmic. However, it has been observed that hNAP-1 carries both a nuclear localization signal and a nuclear export signal consistent with its role as a shuttling protein. Therefore, we incubated cells for 4 h with Leptomycin B at 40 ng/ml. Leptomycin B, an inhibitor of nuclear export, induced nuclear relocalization of hNAP-1 as well as of the hybrid construct hNAP-YFP*.

Recruitment of hNAP-1 at the HIV-1 transcription site

Next, we explored the recruitment of hNAP-1 at the site of HIV-1 transcription. For this purpose, we took advantage of a recently developed cell line that carries an integrated proviral DNA that encodes for a taggable mRNA. The system consists of the insertion of the binding sites of the MS2 phage coat protein into the transcribed RNA (Boireau et al. 2007) and allows visualization of associated cofactors (Molle et al. 2007). This allows co-transcriptional binding of the hybrid MS2-Cherry protein and consequent visualization of the site of HIV-1 transcription (bright red spot in

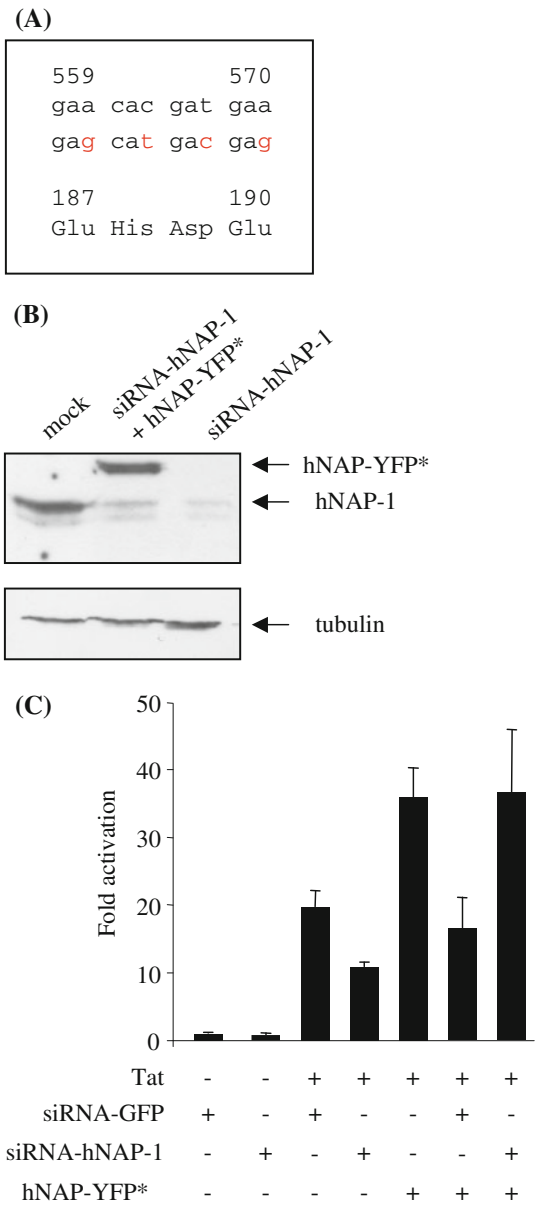

Fig. 1 Characterization of hNAP-YFP*. **a** Sequence of the wild type (*top*) and of the mutated (*bottom*) siRNA target into hNAP-YFP* cDNA. Base changes are in *red*. Amino acid sequence that is not changed is shown below. **b** Immunoblot of endogenous hNAP-1 and transfected hNAP-YFP* in the presence of the siRNA against hNAP-1. Tubulin, loading control. **c** Functional analysis of the hNAP-YFP* construct. A luciferase assay was conducted on HeLa LTR-Luc transactivated by Tat and in the presence of a siRNA against hNAP-1. The siRNA against GFP was used as control that also targets the hNAP-YFP* construct (color figure online)

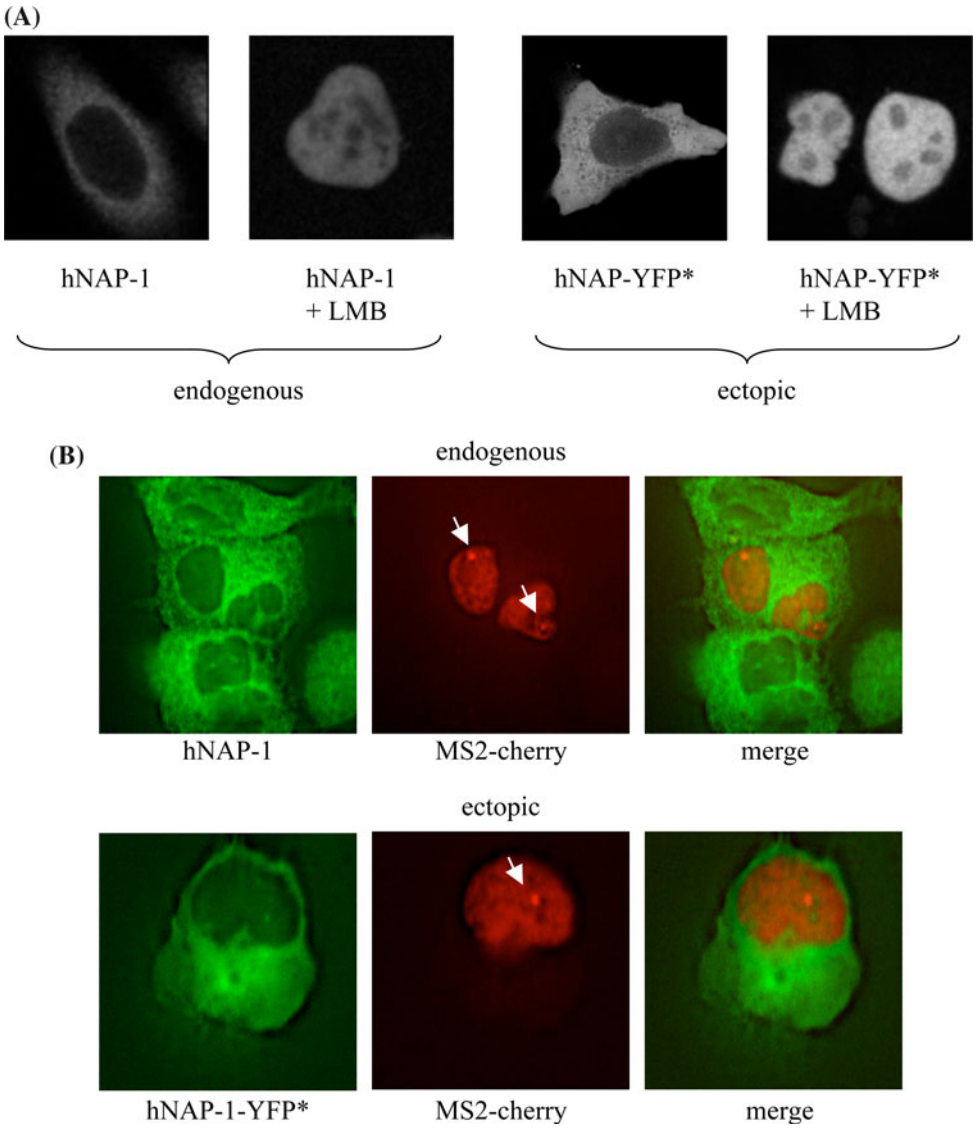

Fig. 2 Subcellular localization of hNAP-1. **a** Subcellular localization of endogenous hNAP-1 and transfected hNAP-YFP* in the presence of Leptomicin B (LMB). HeLa cells were treated as indicated, fixed and incubated with the anti-hNAP-1 antibody. **b** Subcellular localization of endogenous hNAP-1 and transfected hNAP-YFP* (*green*) with respect to the site of HIV-1 transcription (*arrow*) tagged with MS2-Cherry (*red*) (color figure online)

Fig. 2b). Both endogenous hNAP-1 (Fig. 2b, top panels) and transfected hNAP-YFP* (Fig. 2b, bottom panels) were never associated to the HIV-1 transcription site. Hence, the association of hNAP-1 with Tat must occur elsewhere. In order to explore the localization of the association we performed a FRET experiment.

Fluorescence resonance energy transfer

FRET experiments were performed by transfection of HeLa cells with plasmids expressing hNAP-YFP* together with a Tat fusion with the cyan fluorescent protein (Tat-CFP). Fusion proteins of Tat with spectral variants of the GFP at its carboxyl-terminus were previously shown to be transcriptionally competent (Marcello et al. 2001a). As a positive control, we used an engineered in-frame fusion protein between CFP and YFP that is capable of intramolecular FRET in the same experimental conditions (Karpova et al. 2003). As a negative control, we used the MS2-YFPnls fusion protein that localizes to the nucleus when overexpressed (Boireau et al. 2007). In addition, also as a negative control, we used the acid nuclear protein 32B (ANP32B) that forms a complex with the template-activating factor I/Set oncoprotein (TAF-I/Set), which belongs to the NAP-1 family of histone chaperones (Pegoraro et al. 2006). As shown in the histogram of Fig. 3a, FRET measured for the whole cell was significant for the hNAP-YFP*:Tat-CFP pair and was independent on Leptomycin B treatment that increases the concentration of hNAP-YFP* in the nucleus. Consistently, only background FRET was observed in the nucleus both in the presence or absence of Leptomycin B. In order to confirm FRET data and to avoid possible artefacts, we performed an emission spectral analysis with 405 nm laser excitation (Fig. 3b). Also in this case, the hNAP-YFP* and Tat-CFP pair showed the appearance of the FRET emission peak at 524 nm as the

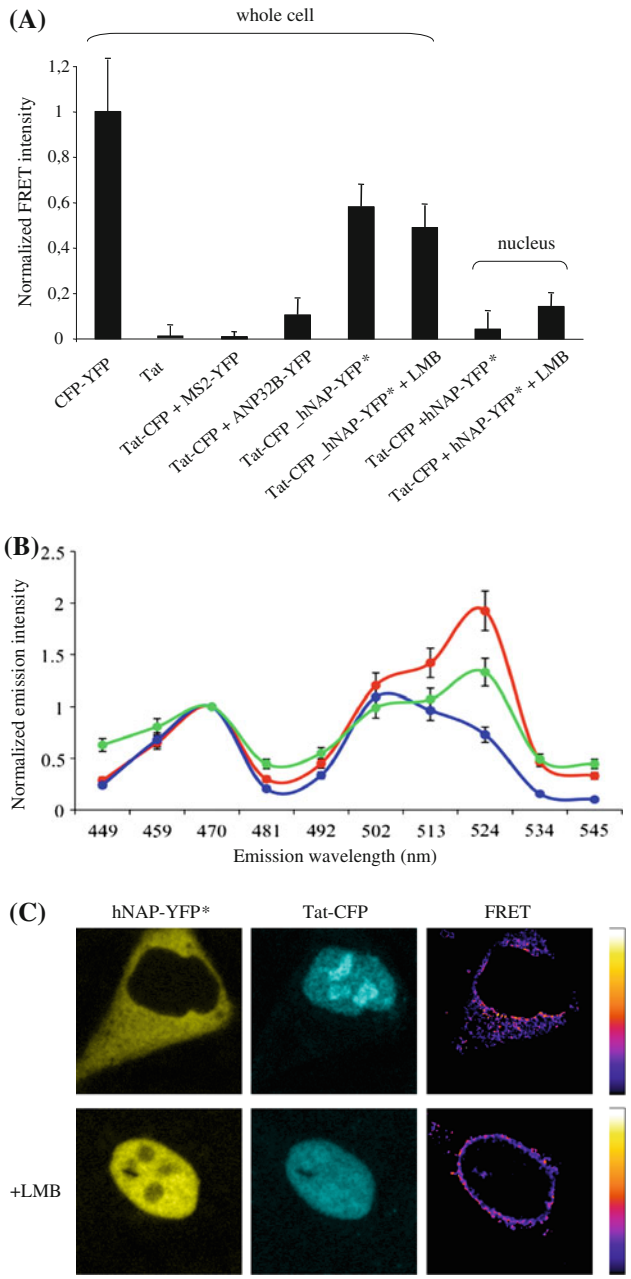

◀ **Fig. 3** **a** Quantification of FRET. Histogram showing the FRET efficiency normalized for the positive control in cells transfected with the indicated constructs: CFP-YFP positive FRET control, Tat-CFP + MS2-YFPnls negative control, Tat-CFP + ANP32-YFP negative control. The measurements were taken for the whole cell, only for the nucleus or in the presence of Leptomycin B. As shown the interaction between Tat-CFP and hNAP-YFP* was significant in the whole cell, both with and without Leptomycin B, but the contribution from the nucleus was irrelevant. **b** Spectral analysis of FRET. Emission spectra at 405 nm excitation of cells transfected with the positive control CFP-YFP (*red*, *top*), the negative control Tat-CFP + MS2-YFP (*blue*, *bottom*) and Tat-CFP + hNap-YFP* (*green*, *middle*). *Y*-axis: emission intensity normalized to the values at 470 nm, *x*-axis: emission wavelengths. **c** FRET experiments showing that the localization of the interaction between Tat and hNAP is in the perinuclear region. HeLa cells where transfected with hNAP-YFP* and Tat-CFP, fixed in paraformaldehyde and subjected to fluorescence microscopy. Relative FRET signal intensity is quantified in the rainbow indicator (from *low/bottom* to *high/top*). Addition of Leptomycin B (*LMB*) changed the localization of hNAP-YFP* as expected but did not change the localization of the FRET signal (*bottom panels*) (color figure online)

positive control CFP-YFP. Finally, we wished to visualize the subcellular localization of the FRET signal. As shown in Fig. 3c, the localization of hNAP-YFP* was cytoplasmic (top left panel) and the localization of Tat-CFP nuclear (middle). A positive FRET signal was evident at the nuclear rim (right). It may be argued that the signal depends simply by partial colocalization of the two proteins. However, when the cells where incubated with Leptomycin B increasing the nuclear concentration of hNAP-YFP* (bottom left panel), FRET signal disappeared from the cytoplasm, in agreement to reduced levels of the acceptor, but remained at the nuclear rim (Fig. 3c, bottom panels). We conclude that hNAP-YFP* and Tat-CFP interact only close to the nuclear membrane.

Structural model of the interaction

Aiming at a structural perspective of the interaction, we constructed a model of the complex starting from the structure of the isolated components using a blind rigid docking procedure. Our FRET data implies that both proteins interact despite the presence of the bulky fluorescent modules that generates a considerable steric hindrance. This is particularly important in the case of the small (86 residues long) Tat protein. To explicitly consider this in our docking trials, we generated and relaxed a structural model of Tat fused to a spectral variant of the GFP protein using MD techniques (Fig. 4a, b). This model was used as the 'ligand' in the docking trials. For the 'receptor', we used the X-ray structure of the yeast homolog of hNAP-1, which shares 81% of identity with the human counterpart for which structural information is not yet available. All the different reciprocal orientations calculated in the docking runs were clustered and the lowest energy member of each cluster was considered as representative. The two best scoring sets corresponded to a symmetry rotation of the hNAP-1 homodimer and can be considered as the same solution. Biochemical analysis indicated that Tat:hNAP-1 binding is mediated by the basic domain of Tat (Vardabasso et al. 2008). Therefore, all docking solutions in which Tat residues from Arg49 to Arg57 were not in contact with the hNAP-1 surface were filtered out. The best docking solutions correspond to structural models that place the basic domain of Tat within the histone-binding site proposed by Park and Luger (2006b).

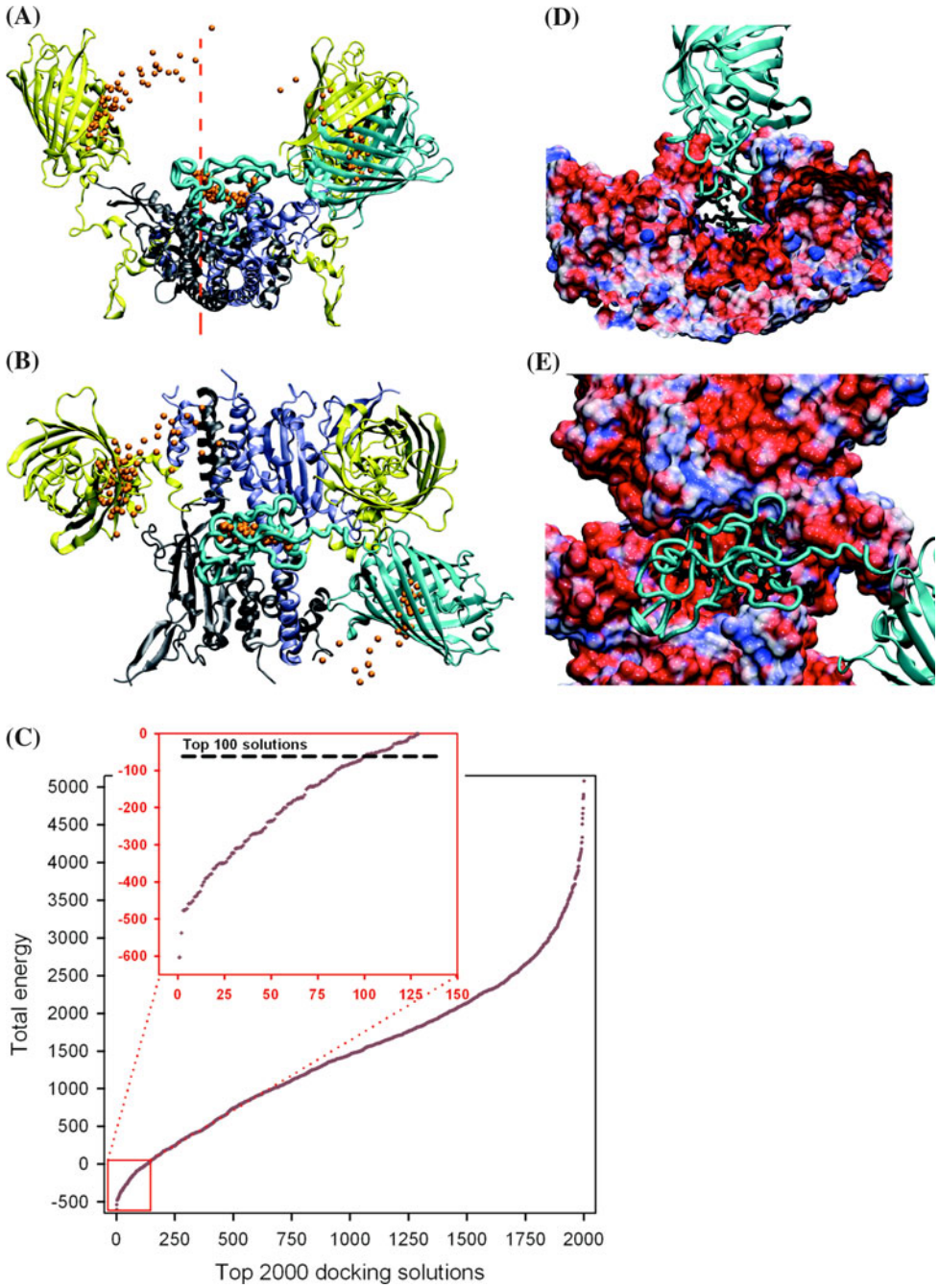

Fig. 4 Structural model of the Tat:hNAP-1 interaction. **a**, **b** *Top* and *side* views of a cartoon representation of the best scoring docking solution. Tat (thick tube) fused to a fluorescent module (cartoon) are depicted in *cyan*. The core structure of the two monomers of the hNAP-1 dimer is colored in *light* and *dark blue*, respectively. The YFP module together with the C-terminal segment of hNAP-1, not determined in the X-ray structure, are shown in *yellow*. The coordinates of these C-terminal segments where obtained from a simulated annealing simulation. Therefore, they have to be considered only as a reasonable conformation included in the figure only to illustrate a possible molecular scenario. *Orange balls* indicate the geometrical centers of Tat and its fused fluorescent module (i.e. two points per docking solution are shown). The symmetry between the two most populated poses is evident from the two clouds of points corresponding to the fluorophore centers. **c** Energy profile of the docking solutions. The inset shows the distribution of the top 100 results. Notice that the binding energy is obtained from an effective force field and has to be taken simply as a scoring function. **d** Molecular electrostatic profiles mapped onto the solvent accessible surface of hNAP-1 (*red* = −10 kT/e, *white* = 0 kT/e, *blue* = +10 kT/e). Residues of the Tat basic domain docked within the acidic pocket of hNAP-1 are shown in *black sticks*. The figure is a cross section on the plane indicated by the *red dashed line* shown in **a**. **e** Top view of **d** (color figure online)

Independent support for the robustness of the docking solution comes from the localization of the best scoring complexes. Figure 4a, b, show the geometric center of the 100 best scoring solutions. Regardless the clustering they all concentrate in the same region of the top model and can be considered as almost equivalent within roughness of the model. The energy profile (Fig. 4c) shows that these first 100 poses include most of the energetically stable solutions. Hence, significantly different docking solutions can be neglected.

The position of Tat into the histone-binding site suggests that it may compete for this pocket. Indeed, the polyarginine tract of Tat shows a nearly linear structure (Pantano and Carloni 2005; Pantano et al. 2006) similar to the conformation of the basic histone tails (Davey et al. 2002).

The basic character of the binding peptides seems to be a fundamental ingredient for binding in sight of the highly acid characteristics of the pocket (Fig. 4d, e).

The conformation of the C-terminal residues of hNAP-1 was not determined in the X-ray structure. Therefore, to evaluate the compatibility of our structural model with the FRET data, we estimated the mean distance from the last residue in the X-ray structure to the fluorophore using a simulated annealing protocol. We obtained a large variability with values ranging from 4 to 7 nm. Nevertheless, when translated this data into our structural model of the complex (illustrated in Fig. 4), it comes out that the maximum expected interfluorophore distance remains always below 9 nm. This indicates that the reciprocal positioning of the two proteins in our model is consistent with the range of distance needed for the two fluorescent modules to perform FRET.

Conclusions

The histone chaperone hNAP-1 is a novel cellular cofactor that significantly enhances HIV-1 Tat-mediated transactivation (Vardabasso et al. 2008). Besides its role as a histone chaperone, hNAP-1 has been shown to interact with several transcription factors, particularly of viral origin. In a yeast two-hybrid screen, hNAP-1 forms a complex with the human papillomavirus transcriptional activator E2 able to activate transcription in vitro (Rehtanz et al. 2004). hNAP-1 binds to the Epstein–Barr virus nuclear antigen 1 (EBNA1) and contributes to EBNA1-mediated transcriptional activation (Holowaty et al. 2003). hNAP-1 also interacts with the Tax protein of the human T-lymphotropic virus 1 (HTLV-1) to promote nucleosome eviction at the HTLV-1 promoter (Sharma and Nyborg 2008). Furthermore, hNAP-1 was also shown to interact with HIV-1 Rev and stimulate its RNA export activity (Cochrane et al. 2009). Interestingly, interactions of hNAP-1 with Tat, Rev and EBNA1 occur all through arginine-rich regions (Cochrane et al. 2009; Holowaty et al. 2003; Vardabasso et al. 2008). Furthermore, functional activity requires the p300 acetyltransferase for HPV E2, HTLV-1 Tax and possibly HIV-1 Tat (Holowaty et al. 2003; Rehtanz et al. 2004; Vardabasso et al. 2008). Cooperative association of hNAP-1 with p300 appears to affect chromatin remodeling, but also the acetyltransferase activity of p300 (Asahara et al. 2002).

Although it is clear that hNAP-1 functions at the level of nucleosome remodeling in some cases, like for example the interaction with Tax (Sharma and Nyborg 2008), it is also evident that this is not its unique mode of action since, for example, the Rev protein typically moves in and out of the nucleus to export viral RNAs (Cochrane et al. 2009). Indeed, hNAP-1 functions also as a chaperone by shuttling histones into the nucleus. In support of this notion, it was found that Drosophila dNAP1 is present in the nucleus during S phase and is predominantly cytoplasmic during G2 phase (Ito et al. 1996). Similar results were reported for the human variant hNAP-2 (Rodriguez et al. 1997). Furthermore, yeast yNAP-1 acts to mediate the interaction between H2A/H2B and karyopherin required for the nuclear import of histones (Mosammaparast et al. 2002). The presence of a nucleus export signal ensures that yNAP-1 is exported once histones are released in the nucleus (Miyaji-Yamaguchi et al. 2003).

In this work, we addressed the question of where the functional interaction between hNAP-1 and HIV-1 occurred. To this end, we took advantage of the possibility of visualizing viral transcription and the associated factors by tagging the HIV-1 genome with the binding sites of the MS2 protein as described previously (Boireau et al. 2007; Molle et al. 2007). However, although the signal marking the transcription site was clearly evident, no recruitment of hNAP-1 was observed. This finding suggests that the functional interaction between Tat and hNAP-1 occurs elsewhere or is extremely transient at the transcription site. The latter hypothesis appears unlikely since (1) we were able to detect several Tat interactors at the HIV-1 transcription site by this method, including Cyclin T1, p300 and CDK9 (Boireau et al. 2007; Molle et al. 2007); (2) this method, based on tagging nascent RNAs, marks the sites where active transcription is taking place, where nucleosomes are actively remodeled (Marcello et al. 2001b).

FRET analysis shows that the interaction of Tat with hNAP-1 occurs within the cell but is limited to the nuclear rim. This information is consistent with a role of hNAP-1 in Tat shuttling similar to what has been proposed for histones (Park and Luger 2006a). Structural modeling of the complex between hNAP-1 and HIV-1 Tat suggests that Tat binds within the same binding site used by histone tails. Unfortunately, the biological/biochemical information

available does not provide the necessary tools to construct a reliable model at the single residue level. However, the incorporation of restrictions coming from the FRET data (excluded volume of the ligand, maximum inter fluorophore distance) together with previously biochemical data (Vardabasso et al. 2008) allow the theoretical method to furnish a good indication of the binding region of the two molecules.

Nuclear import of Tat is a non-classical energy-dependent process selectively mediated by importin β (Efthymiadis et al. 1998; Truant and Cullen 1999). This involves the molecular recognition of the arginine-rich motif of Tat by importin β, with no apparent need for the adapter protein importin α. Subsequently, importin β interacts with nuclear pore complexes and mediates the translocation of Tat into the nucleus. We found that the interaction of hNAP-1 with Tat occurs on the nuclear rim and involves the same domain also bound by Importin β. It is possible that hNAP-1 helps Tat interacting with Importin β for nuclear import. Accordingly, it has been shown that yeast yNAP1 mediates the interaction between H2A/H2B and the Kap114p karyopherin and this interaction is necessary for the nuclear import of histones (Mosammaparast et al. 2002). In light of these observations, it will be important to dissect the mechanism of Tat import and release in the nucleus to provide a better understanding of the process and possible new targets for antiviral therapy.

Acknowledgments We thank Edouard Bertrand (IGMM, Montpellier) for the use of the microscopy facility and for advice. This work (AM) was supported in part by a HFSP Young Investigators Grant, by the Italian FIRB program of the Ministero dell'Istruzione, Università e Ricerca of Italy, by the European Community FP6 STREP n. 012182 and by the AIDS Program of the Istituto Superiore di Sanità of Italy. PD and SP were supported by ANII—Agencia Nacional de Investigación e Innovación, Programa de Apoyo Sectorial a la Estrategia Nacional de Innovación—INNOVA URUGUAY (Agreement no. DCI—ALA/2007/19.040 between Uruguay and the European Commission and FCE_60/2007).

References

Asahara H, Tartare-Deckert S, Nakagawa T, Ikehara T, Hirose F, Hunter T, Ito T, Montminy M (2002) Dual roles of p300 in chromatin assembly and transcriptional activation in cooperation with nucleosome assembly protein 1 in vitro. Mol Cell Biol 22:2974–2983

Benkirane M, Chun RF, Xiao H, Ogryzko VV, Howard BH, Nakatani Y, Jeang KT (1998) Activation of integrated provirus requires histone acetyltransferase. p300 and P/CAF are coactivators for HIV-1 Tat. J Biol Chem 273:24898–24905

Berkhout B, Silverman RH, Jeang KT (1989) Tat trans-activates the human immunodeficiency virus through a nascent RNA target. Cell 59:273–282

Boireau S, Maiuri P, Basyuk E, de la Mata M, Knezevich A, Pradet-Balade B, Backer V, Kornblihtt A, Marcello A, Bertrand E (2007) The transcriptional cycle of HIV-1 in real-time and live cells. J Cell Biol 179:291–304

Bres V, Tagami H, Peloponese JM, Loret E, Jeang KT, Nakatani Y, Emiliani S, Benkirane M, Kiernan RE (2002) Differential acetylation of Tat coordinates its interaction with the co-activators cyclin T1 and PCAF. EMBO J 21:6811–6819

Bres V, Gomes N, Pickle L, Jones KA (2005) A human splicing factor, SKIP, associates with P-TEFb and enhances transcription elongation by HIV-1 Tat. Genes Dev 19:1211–1226

Case DA, Darden TA, Cheatham III TE, Simmerling CL, Wang J, Duke RE, Lou R, Merz KM, Wang B, Pearlman DA, Crowley M, Brozell S, Tsui V, Gohlke H, Mongan J, Hornak V, Cui G, Beroza P, Schafmeister C, Caldwell JW, Ross WS, Kollman PA (2004) Amber 8.0 (5.0). University of California, San Francisco

Cochrane A, Murley LL, Gao M, Wong R, Clayton K, Brufatto N, Canadien V, Mamelak D, Chen T, Richards D, Zeghouf M, Greenblatt J, Burks C, Frappier L (2009) Stable complex formation between HIV Rev and the nucleosome assembly protein, NAP1, affects Rev function. Virology 388:103–111

Cook PR (1999) The organization of replication and transcription. Science 284:1790–1795

Cornell WD, Cieplak P, Bayly CI, Gould IR, Merz KM, Ferguson DM, Spellmayer DC, Fox T, Caldwell JW, Kollman PA (1995) A second generation force field for the simulation of proteins, nucleic acids, and organic molecules. J Am Chem Soc 117:5179–5197

Davey CA, Sargent DF, Luger K, Maeder AW, Richmond TJ (2002) Solvent mediated interactions in the structure of the nucleosome core particle at 1.9 a resolution. J Mol Biol 319:1097–1113

Day RN, Periasamy A, Schaufele F (2001) Fluorescence resonance energy transfer microscopy of localized protein interactions in the living cell nucleus. Methods 25:4–18

Dorr A, Kiermer V, Pedal A, Rackwitz HR, Henklein P, Schubert U, Zhou MM, Verdin E, Ott M (2002) Transcriptional synergy between Tat and PCAF is dependent on the binding of acetylated Tat to the PCAF bromodomain. EMBO J 21:2715–2723

du Chene I, Basyuk E, Lin YL, Triboulet R, Knezevich A, Chable-Bessia C, Mettling C, Baillat V, Reynes J, Corbeau P, Bertrand E, Marcello A, Emiliani S, Kiernan R, Benkirane M (2007) Suv39H1 and HP1gamma are responsible for chromatin-mediated HIV-1 transcriptional silencing and post-integration latency. EMBO J 26:424–435

Efthymiadis A, Briggs LJ, Jans DA (1998) The HIV-1 Tat nuclear localization sequence confers novel nuclear import properties. J Biol Chem 273:1623–1628

Feige JN, Sage D, Wahli W, Desvergne B, Gelman L (2005) PixFRET, an ImageJ plug-in for FRET calculation that can accommodate variations in spectral bleed-throughs. Microsc Res Tech 68:51–58

Groth A, Rocha W, Verreault A, Almouzni G (2007) Chromatin challenges during DNA replication and repair. Cell 128:721–733

Haushalter KA, Kadonaga JT (2003) Chromatin assembly by DNA-translocating motors. Nat Rev Mol Cell Biol 4:613–620

Hawkins GD, Cramer CJ, Truhlar DG (1996) Parametrized models of aqueous free energies of solvation based on pairwise descreening of solute atomic charges from a dielectric medium. J Phys Chem 100:19824–19839

Holowaty MN, Zeghouf M, Wu H, Tellam J, Athanasopoulos V, Greenblatt J, Frappier L (2003) Protein profiling with Epstein-Barr nuclear antigen-1 reveals an interaction with the herpesvirus-associated ubiquitin-specific protease HAUSP/USP7. J Biol Chem 278:29987–29994

Hottiger MO, Nabel GJ (1998) Interaction of human immunodeficiency virus type 1 Tat with the transcriptional coactivators p300 and CREB binding protein. J Virol 72:8252–8256

Ishimi Y, Kikuchi A (1991) Identification and molecular cloning of yeast homolog of nucleosome assembly protein I which facilitates nucleosome assembly in vitro. J Biol Chem 266:7025–7029

Ito T, Bulger M, Kobayashi R, Kadonaga JT (1996) Drosophila NAP-1 is a core histone chaperone that functions in ATP-facilitated assembly of regularly spaced nucleosomal arrays. Mol Cell Biol 16:3112–3124

Kaehlcke K, Dorr A, Hetzer-Egger C, Kiermer V, Henklein P, Schnoelzer M, Loret E, Cole PA, Verdin E, Ott M (2003) Acetylation of Tat defines a cyclinT1-independent step in HIV transactivation. Mol Cell 12:167–176

Karpova TS, Baumann CT, He L, Wu X, Grammer A, Lipsky P, Hager GL, McNally JG (2003) Fluorescence resonance energy transfer from cyan to yellow fluorescent protein detected by acceptor photobleaching using confocal microscopy and a single laser. J Microsc 209:56–70

Kellogg DR, Kikuchi A, Fujii-Nakata T, Turck CW, Murray AW (1995) Members of the NAP/SET family of proteins interact specifically with B-type cyclins. J Cell Biol 130:661–673

Kiernan RE, Vanhulle C, Schiltz L, Adam E, Xiao H, Maudoux F, Calomme C, Burny A, Nakatani Y, Jeang KT, Benkirane M, Van Lint C (1999) HIV-1 tat transcriptional activity is regulated by acetylation. EMBO J 18:6106–6118

Kouzarides T (2007) Chromatin modifications and their function. Cell 128:693–705

Levchenko V, Jackson V (2004) Histone release during transcription: NAP1 forms a complex with H2A and H2B and facilitates a topologically dependent release of H3 and H4 from the nucleosome. Biochemistry 43:2359–2372

Li B, Carey M, Workman JL (2007) The role of chromatin during transcription. Cell 128:707–719

Luger K, Mader AW, Richmond RK, Sargent DF, Richmond TJ (1997) Crystal structure of the nucleosome core particle at 2.8 A resolution. Nature 389:251–260

Lusic M, Marcello A, Cereseto A, Giacca M (2003) Regulation of HIV-1 gene expression by histone acetylation and factor recruitment at the LTR promoter. EMBO J 22:6550–6561

Marcello A, Cinelli RA, Ferrari A, Signorelli A, Tyagi M, Pellegrini V, Beltram F, Giacca M (2001a) Visualization of in vivo direct interaction between HIV-1 TAT and human cyclin T1 in specific subcellular compartments by fluorescence resonance energy transfer. J Biol Chem 276:39220–39225

Marcello A, Zoppe M, Giacca M (2001b) Multiple modes of transcriptional regulation by the HIV-1 Tat transactivator. IUBMB Life 51:175–181

Marcello A, Ferrari A, Pellegrini V, Pegoraro G, Lusic M, Beltram F, Giacca M (2003) Recruitment of human cyclin T1 to nuclear bodies through direct interaction with the PML protein. EMBO J 22:2156–2166

Marcello A, Lusic M, Pegoraro G, Pellegrini V, Beltram F, Giacca M (2004) Nuclear organization and the control of HIV-1 transcription. Gene 326:1–11

Marzio G, Tyagi M, Gutierrez MI, Giacca M (1998) HIV-1 tat transactivator recruits p300 and CREB-binding protein histone acetyltransferases to the viral promoter. Proc Natl Acad Sci USA 95:13519–13524

Miyaji-Yamaguchi M, Kato K, Nakano R, Akashi T, Kikuchi A, Nagata K (2003) Involvement of nucleocytoplasmic shuttling of yeast Nap1 in mitotic progression. Mol Cell Biol 23:6672–6684

Mizuguchi G, Shen X, Landry J, Wu WH, Sen S, Wu C (2004) ATP-driven exchange of histone H2AZ variant catalyzed by SWR1 chromatin remodeling complex. Science 303:343–348

Molle D, Maiuri P, Boireau S, Bertrand E, Knezevich A, Marcello A, Basyuk E (2007) A real-time view of the TAR:Tat:P-TEFb complex at HIV-1 transcription sites. Retrovirology 4:36

Mosammaparast N, Ewart CS, Pemberton LF (2002) A role for nucleosome assembly protein 1 in the nuclear transport of histones H2A and H2B. EMBO J 21:6527–6538

Okuwaki M, Kato K, Shimahara H, Tate S, Nagata K (2005) Assembly and disassembly of nucleosome core particles containing histone variants by human nucleosome assembly protein I. Mol Cell Biol 25:10639–10651

Ott M, Schnolzer M, Garnica J, Fischle W, Emiliani S, Rackwitz HR, Verdin E (1999) Acetylation of the HIV-1 Tat protein by p300 is important for its transcriptional activity. Curr Biol 9:1489–1492

Pagans S, Pedal A, North BJ, Kaehlcke K, Marshall BL, Dorr A, Hetzer-Egger C, Henklein P, Frye R, McBurney MW, Hruby H, Jung M, Verdin E, Ott M (2005) SIRT1 regulates HIV transcription via Tat deacetylation. PLoS Biol 3:e41

Pantano S (2008) In silico description of fluorescent probes in vivo. J Mol Graph Model 27:563–567

Pantano S, Carloni P (2005) Comparative analysis of HIV-1 Tat variants. Proteins 58:638–643

Pantano S, Marcello A, Ferrari A, Gaudiosi D, Sabo A, Pellegrini V, Beltram F, Giacca M, Carloni P (2006) Insights on HIV-1 Tat:P/CAF bromodomain molecular recognition from in vivo experiments and molecular dynamics simulations. Proteins 62:1062–1073

Park YJ, Luger K (2006a) Structure and function of nucleosome assembly proteins. Biochem Cell Biol 84:549–558

Park YJ, Luger K (2006b) The structure of nucleosome assembly protein 1. Proc Natl Acad Sci USA 103:1248–1253

Park YJ, Chodaparambil JV, Bao Y, McBryant SJ, Luger K (2005) Nucleosome assembly protein 1 exchanges histone H2A–H2B dimers and assists nucleosome sliding. J Biol Chem 280:1817–1825

Pegoraro G, Marcello A, Myers MP, Giacca M (2006) Regulation of adeno-associated virus DNA replication by the cellular TAF-I/set complex. J Virol 80:6855–6864

Peloponese JM Jr, Gregoire C, Opi S, Esquieu D, Sturgis J, Lebrun E, Meurs E, Collette Y, Olive D, Aubertin AM, Witvrow M, Pannecouque C, De Clercq E, Bailly C, Lebreton J, Loret EP (2000) 1H–13C nuclear magnetic resonance assignment and structural characterization of HIV-1 Tat protein. C R Acad Sci III 323:883–894

Ping YH, Rana TM (2001) DSIF and NELF interact with RNA polymerase II elongation complex and HIV-1 Tat stimulates P-TEFb-mediated phosphorylation of RNA polymerase II and DSIF during transcription elongation. J Biol Chem 276:12951–12958

Rehtanz M, Schmidt HM, Warthorst U, Steger G (2004) Direct interaction between nucleosome assembly protein 1 and the papillomavirus E2 proteins involved in activation of transcription. Mol Cell Biol 24:2153–2168

Ritchie DW (2008) Recent progress and future directions in protein-protein docking. Curr Protein Pept Sci 9:1–15

Rodriguez P, Munroe D, Prawitt D, Chu LL, Bric E, Kim J, Reid LH, Davies C, Nakagama H, Loebbert R, Winterpacht A, Petruzzi MJ, Higgins MJ, Nowak N, Evans G, Shows T, Weissman BE, Zabel B, Housman DE, Pelletier J (1997) Functional characterization of human nucleosome assembly protein-2 (NAP1L4) suggests a role as a histone chaperone. Genomics 44:253–265

Ryckaert JP, Ciccotti G, Berendsen HJ (1977) Numerical integration of the Cartesian equations of motion of a system with constraints: molecular dynamics of n-Alkanes. J Comput Phys 23:327–341

Sharma N, Nyborg JK (2008) The coactivators CBP/p300 and the histone chaperone NAP1 promote transcription-independent nucleosome eviction at the HTLV-1 promoter. Proc Natl Acad Sci USA 105:7959–7963

Sutherland H, Bickmore WA (2009) Transcription factories: gene expression in unions? Nat Rev Genet 10:457–466

Truant R, Cullen BR (1999) The arginine-rich domains present in human immunodeficiency virus type 1 Tat and Rev function as direct importin beta-dependent nuclear localization signals. Mol Cell Biol 19:1210–1217

Tsui V, Case DA (2000) Theory and applications of the generalized Born solvation model in macromolecular simulations. Biopolymers 56:275–291

Vardabasso C, Manganaro L, Lusic M, Marcello A, Giacca M (2008) The histone chaperone protein Nucleosome Assembly Protein-1 (hNAP-1) binds HIV-1 Tat and promotes viral transcription. Retrovirology 5:8

Voss TC, Demarco IA, Day RN (2005) Quantitative imaging of protein interactions in the cell nucleus. Biotechniques 38:413–424

Wachter RM, Elsliger MA, Kallio K, Hanson GT, Remington SJ (1998) Structural basis of spectral shifts in the yellow-emission variants of green fluorescent protein. Structure 6:1267–1277

Walter PP, Owen-Hughes TA, Cote J, Workman JL (1995) Stimulation of transcription factor binding and histone displacement by nucleosome assembly protein 1 and nucleoplasmin requires disruption of the histone octamer. Mol Cell Biol 15:6178–6187

Xie B, Invernizzi CF, Richard S, Wainberg MA (2007) Arginine methylation of the human immunodeficiency virus type 1 Tat protein by PRMT6 negatively affects Tat Interactions with both cyclin T1 and the Tat transactivation region. J Virol 81:4226–4234